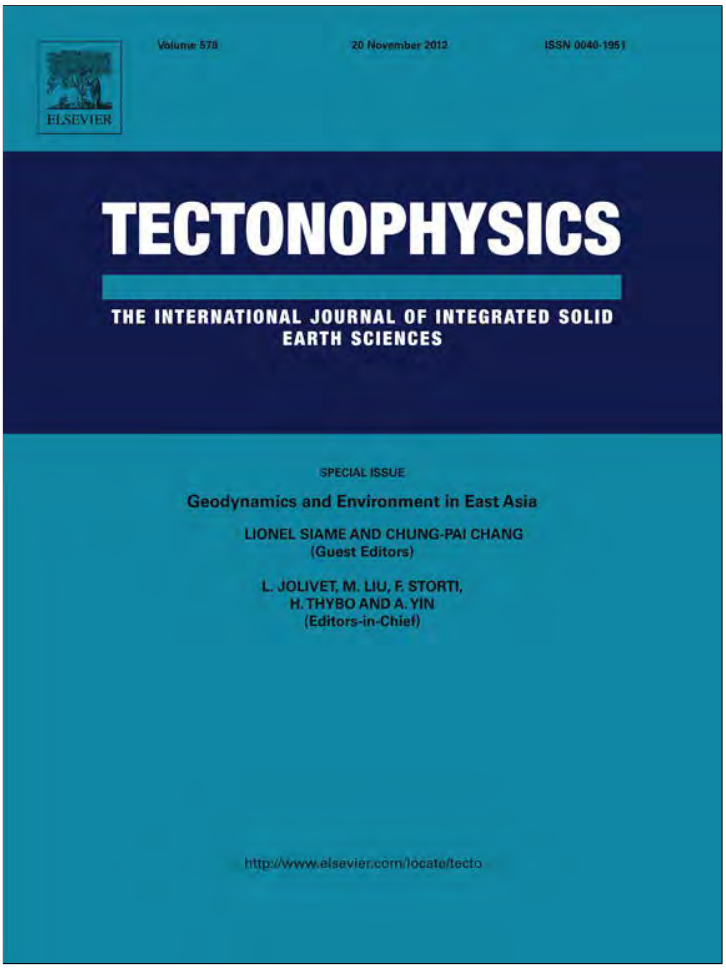

Tectonophysics 578 (2012) 107–116

Contents lists available at SciVerse ScienceDirect

Tectonophysics

journal homepage: www.elsevier.com/locate/tecto

Subduction-continent collision in southwestern Taiwan and the 2010 Jiashian earthquake sequence

Ruey-Juin Rau [a,*], Jian-Cheng Lee [b], Kuo-En Ching [c], Yuan-Hsi Lee [d], Timothy B. Byrne [e], Rong-Yuh Chen [f]

[a] Department of Earth Sciences, National Cheng Kung University, Tainan, Taiwan
[b] Institute of Earth Sciences, Academia Sinica, Taipei, Taiwan
[c] Department of Geomatics, National Cheng Kung University, Tainan, Taiwan
[d] Department of Earth and Environmental Sciences, National Chung Cheng University, Chia-Yi, Taiwan
[e] Center for Integrative Geosciences, University of Connecticut, USA
[f] Seismological Center, Central Weather Bureau, Taipei, Taiwan

ARTICLE INFO

Article history:
Received 24 November 2010
Received in revised form 14 July 2011
Accepted 13 September 2011
Available online 1 October 2011

Keywords:
Southern Taiwan
2010 Jiashian earthquake sequence
Local earthquake tomography
Focal mechanisms and stress tensor
Lateral compression
Oblique subduction

ABSTRACT

We integrated a regional tomography model, 20-year seismicity and earthquake focal mechanisms of the 4 March 2010 M_L 6.4 Jiashian earthquake source region to delineate the seismogenic structure and mechanics of a relatively rare damaging inland earthquake that occurred in the southwestern fold-and-thrust belt of Taiwan. The main shock of the Jiashian earthquake occurred at a depth of 23 km beneath the slate belt of the southern Central Range with a sinistral thrust mechanism. Based on seismic tomography and seismicity, the Jiashian earthquake sequence occurred in the Chishan transfer fault zone, which we interpret to be located near the transition zone between the subducted Eurasian plate to the south and the arc–continent Taiwan collision to the north. The distribution of the Jiashian aftershocks define a WNW-ESE striking fault plane that dips 30–40° NNE which is consistent with the optimal fault plane of the GPS-derived coseismic slip model. Focal mechanisms and inverted stress results of the earthquake sequence indicate both thrust and strike–slip motions with the maximum compressive stress at nearly 90° to the regional compressive stress and thus sub-parallel to the strike of the Taiwan orogen. We propose that the 2010 Jiashian earthquake resulted from rupturing of a buried oblique fault within the Chishan transfer fault zone at the subduction–collision transition zone in southern Taiwan. The orogen-parallel P-axis of the 2010 Jiashian earthquake represents collision-related lateral compression, although a local stress deviation is also possible.

1. Introduction

The 4 March 2010 M_L 6.4 Jiashian earthquake is the largest inland earthquake in the southwestern fold-and-thrust belt of Taiwan since the 1964 M 6.3 Paiho earthquake (Fig. 1). No deaths, but 96 people injuries were reported. Two high speed trains were disrupted at the time of quake due to ground shaking and as a result, more than 2300 people were evacuated from the trains. The Jiashian earthquake occurred ~17 km southeast of the Jiashian township (at 23.08°N of Latitude and 120.59°E of Longitude) with a focal depth of ~23 km, beneath the slate belt of the southern Central Range (Fig. 1). Both BATS (Broadband Array in Taiwan for Seismology), USGS and Global CMT (Centroid Moment Tensor) solutions indicate a sinistral thrust mechanism (P-axis trending NNE–SSW). The fault plane most likely strikes NW–SE and dips 30–40° to the NE, judging from the aftershock distribution and the GPS coseismic source model (Ching et al., 2011). Ching et al. (2011) used coseismic surface displacements from 139 continuous GPS stations to solve fault geometry and slip distribution on the fault plane. They suggested that the 2010 earthquake ruptured and reactivated the NW-striking Chishan transfer zone, which represents a step-over of the major NNE-trending thrust system in fold-and-thrust belt. They further suggested that the fault revealed a listric shape of NE-dipping lateral ramp with oblique slip. However, Ching et al. (2011) did not discuss much about the mechanism and the regional crustal/seismic structures responsible for the 2010 earthquake.

The NW–SE fault strike of the 2010 earthquake deviates ~70–90° from the NNE trend of major geological structures in the Taiwan mountain belt, which have caused numerous earthquakes to occur in the adjacent region during the past decades (Figs. 1 and 2). Instead, the NW–SE trending fault represents the less predominant strike–slip transfer faults in the fold-and-thrust belt, which have produced occasional large hazardous earthquakes in the past decade, e.g., the 1906 M 7.1 Meishan earthquake and the 1946 M 6.9 Hsinhua earthquake (Fig. 1). This leads us to address the following questions. What is the geological structure accountable for the 2010 Jiashian earthquake, which appears to be one of these NW–SE transfer faults? Is it related to any of the surface geologically mapped fault, or is it associated with

* Corresponding author at: Department of Earth Sciences, National Cheng Kung University, Tainan, 701, Taiwan. Tel.: +886 6 2757575 65425; fax: +886 6 2740285.
E-mail address: raurj@mail.ncku.edu.tw (R.-J. Rau).

0040-1951/$ – see front matter © 2011 Elsevier B.V. All rights reserved.
doi:10.1016/j.tecto.2011.09.013

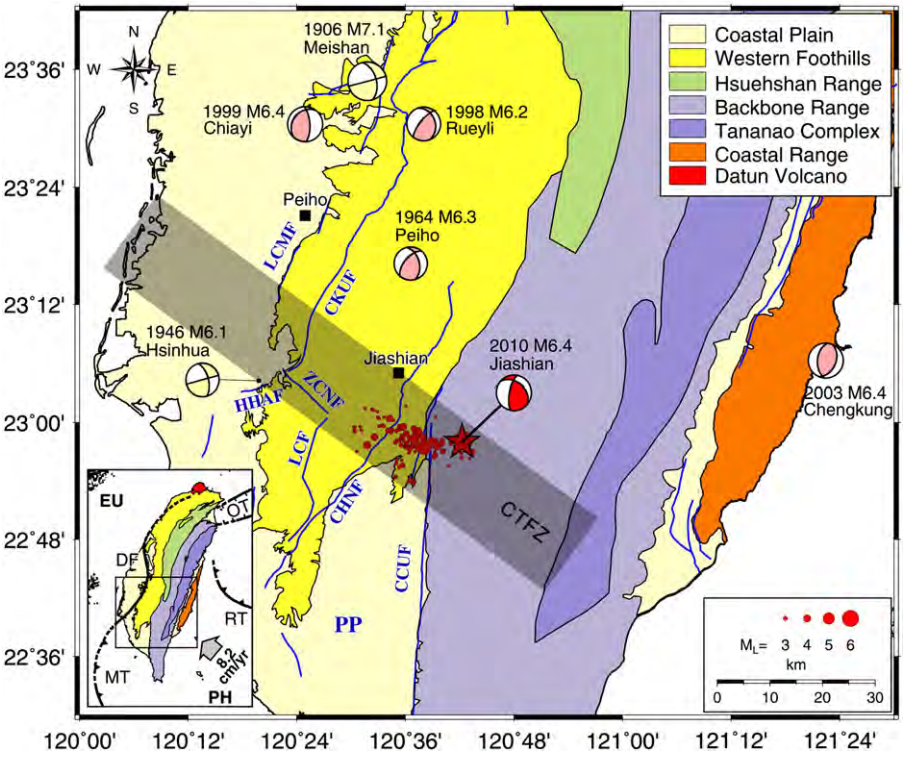

Fig. 1. Map of southern Taiwan showing the locations of 2010 M_L 6.4 Jiashian earthquake sequences (solid red circles) and M>6.0 damaging earthquakes since 1900. Magnitude for the Jiashian earthquake sequences is scaled at the lower right. The Jiashian mainshock is shown as a red star and its mechanism is indicated by the USGS CMT solution. Focal mechanisms are plotted on lower hemisphere, equal-area projection. Active faults are shown as blue lines. Insert shows regional tectonic setting of Taiwan. The vector of relative motion between the Philippine Sea plate and the Eurasian plate is shown by the arrow (Yu et al., 1997). Black rectangle denotes the study area. EU: Eurasian plate; PH: Philippine Sea plate; PP: Pingtung plain; LCMF: Liuchia–Muchiliao fault; CKUF: Chukou fault; HHAF: Hsinhua fault; ZCNF: Zuochen fault; LCF: Lungchuan fault; CHNF: Chishan fault; CCUF: Chaochou fault; CTFZ: Chishan transfer fault zone (shown as a shaded zone); MT: Manila trench; RT: Ryukyu trench; DF: Deformation front; OT: Okinawa trough.

a concealed blind fault? What is the mechanism responsible for the NW–SE-striking and NNE–SSW trending P-axis Jiashian earthquake? What is the regional crustal/seismic structure responsible for the occurrence of the Jiashian earthquake? To address these questions, we evaluated seismicity and determined focal mechanisms for earthquakes from nearly the last two decades, together with seismic tomography model to examine the seismogenic structures and the stress state in the areas surrounding the epicentral area and compared them to the seismic observations of the 2010 Jiashian earthquake sequence.

2. Tectonic setting of southwestern Taiwan

Taiwan provides a classic, although relatively small, mountain belt owing to plate convergence between Eurasia and the Philippine Sea plate, especially the ongoing arc–continent collision began since about 4–5 Ma (e.g., Chi and Huang, 1981; Suppe, 1981, 1984; Teng, 1979). The Taiwan mountain belt, extending about 400 km long and 150 km wide, exhibits a major NNE structural grain, which is approximately perpendicular to the NW-direction of plate convergence (319°). Global plate reconstruction and GPS data indicate a rate of 7 and 8.2 cm/yr, respectively (Seno, 1977; Seno et al., 1993; Yu et al., 1997) (Fig. 1). Due to the two opposing subduction in the southern and northern parts of Taiwan and slightly oblique plate convergence, the growth of the Taiwan mountain belt shows propagation from north to south (Suppe, 1984). At the present, the northern Taiwan is largely under extension or transtension tectonic stress regime as expressed by the N–S opening of the Okinawa Trough and collision-induced clockwise rotation in the plate corner (e.g., Hu et al., 1996; Rau et al., 2008; Teng and Lee, 1996). By contrast, the contraction of arc–continent collision affects both central and southern Taiwan, in particular in the fold-and-thrust belt. Further south, the Eurasian slab (South China Sea) subducts eastward along the Manila trench striking approximately parallel to the structural trend of southern Taiwan.

The fold-and-thrust belt in the western foothills of Taiwan shows a general NNE-trending zone of 300-km long and 20–30 km wide, which is composed of slightly folded pre- and syn-collision sedimentary strata form Miocene and Pliocene marine deposits to Quaternary terrestrial sediments. The structure of the belt is mainly characterized by a series of sub-parallel west-verging imbricate thrusts. Some of the thrusts are considered seismically highly active, especially in the frontal thrust zone. A recent example is the 1999 M_w 7.6 Chi-Chi earthquake, which ruptured the Chelungpu fault, a major thrust in the mountain front in central western Taiwan. In addition to these major mountain-parallel thrust faults, a few obliquely-striking transfer fault zones have been proposed and discussed in the past decades (e.g., Deffontaines et al., 1994). The transfer zones, however, are more subtle in the field compared to the major thrust faults; and evaluating the earthquake potential for these transfer fault zones has remained difficult, although they have been considered to be seismically active. For instance, intense micro-seismicity clearly occurred along the Sanyi–Puli transfer fault zone in northwestern Taiwan (Wu and Rau, 1998), although no solid evidence of field outcrops has been reported.

The study area, southwestern Taiwan, is located in the subduction-to-collision transition zone, which is composed of three major geological/structural domains. The east domain is the Backbone Range, comprised mainly of Oligocene to Miocene fine-grained, low-grade metamorphic slates and meta-sandstones. Structures of the Backbone Range include ductile folds and cleavages, and superimposed brittle faults. The northwest domain represents the southern

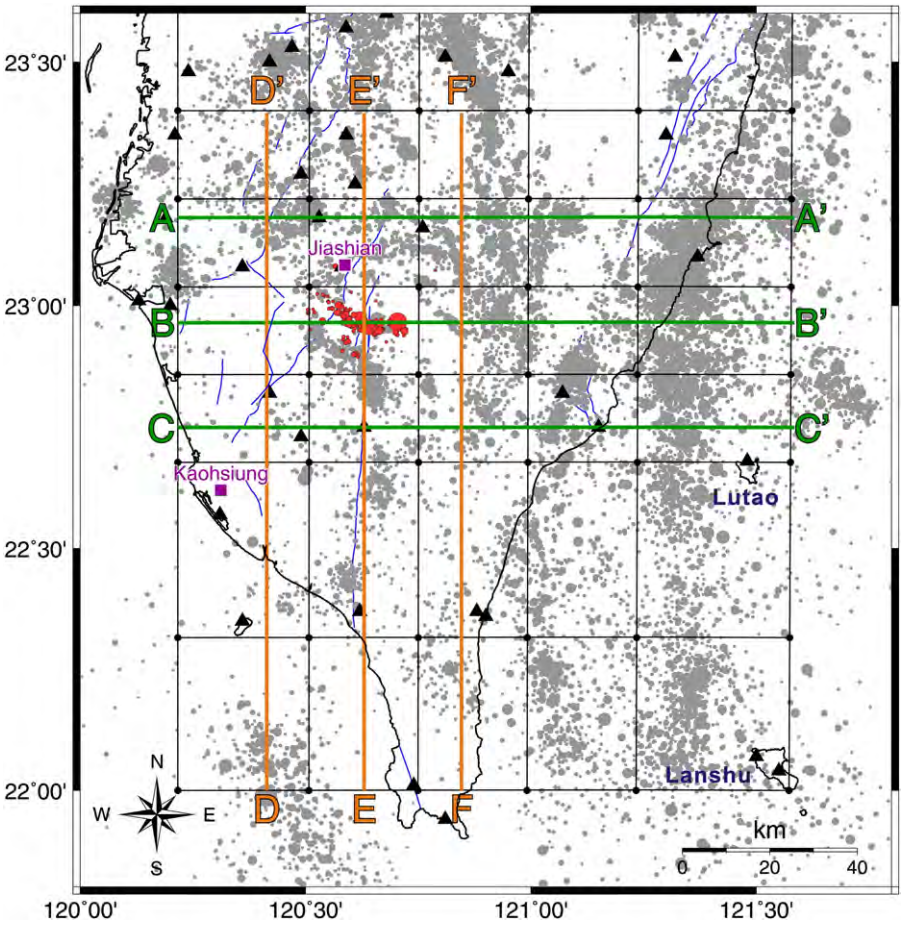

Fig. 2. Map of southern Taiwan showing the grid configurations (only southern Taiwan grids are shown) used in the 3D velocity inversion (Rau and Wu, 1995) and the 2010 M_L 6.4 Jiashian earthquake sequence (red circles) and the M_L>2.5 background seismicity (gray circles) occurred between 1 January 1991 and 31 March 2010. Solid triangles are the CWBSN seismic stations. The earthquakes are relocated by the 3D velocity model. Active faults are shown as blue lines. The nodes, the points where the lines crossed, are shown as solid circles. Profiles AA′–FF′ indicate the locations of the tomographic profiles shown in Figs. 3 and 4.

tip of the fold-and-thrust belt and consists of Miocene shallow marine sandstone and shale and Plio-Pleistocene mudstones, totaling about 5-km in thickness. The sediments are interpreted to be part of the paleo foreland basin that formed as the lithosphere flexed due to the tectonic loading by the Central Range (Lin and Watts, 2002). The southwest domain is a large alluvial plain, the Pingtung plain, located in the southern end of the Western Foothills. The Pingtung plain is composed of late Quaternary marine to fluvial sediments, including fluvial deposits and coastal to estuarine sandstone and mudstone (e.g., Shyu et al., 2005).

Several major faults in SW Taiwan have been identified based on geological field investigations, geomorphologic analyses, and geophysical surveying (Fig. 1). In the northern part, the Chukou fault (CKUF, the southern extension of the Chelungpu fault, the causative fault of the 1999 M 7.6 Chi-Chi earthquake) and the Liuchia–Muchiliao fault (LCMF) together form an imbricate thrust system (Yang et al., 2006) in the frontal thrust zone. Besides these two above active faults, active blind thrust appears to be developing further west under the southwestern Coastal Plain based on crustal deformation and drainage pattern analyses (Yang et al., 2007). Connecting the southern end of the Chukou fault to the southeast is the Lungchuan fault (LCF). However, these two major thrust faults are separated by the N130°E-striking left-lateral Zuochen fault (ZCNF). The Zuochen fault, which is located within the previously proposed Chishan transfer fault zone, is one of several obliquely-striking transfer structures in western Taiwan (Deffontaines et al., 1994, 1997; Lacombe et al., 1999, 2001). Further south, the N–S trending 80-km long Chaochou fault separates the Pingtung alluvial plain and the Central Range (Wiltschko et al., 2010). Recent GPS data indicated that the Chaochou fault probably moved as a reverse fault with sinistral motion during the interseismic period (Ching et al., 2007). West of the Chaochou fault, the NE–SW trending Chishan fault is a major fault in the Western Foothills and is interpreted as a reverse fault with a minor right-lateral component (e.g., Ching et al., 2007; Lacombe et al., 2001). A shortening rate of ~14 mm/yr across the Chishan fault was inferred from the interseismic GPS velocity gradient (Ching et al., 2007).

3. Data and procedures of analyses

We analyzed a tomography model, seismicity and earthquake focal mechanisms in the study area. More than 17,200 $M \geq 2.5$ earthquakes recorded by Central Weather Bureau Seismic Network (CWBSN) from 1991 to 2010 were selected, and the earthquakes were relocated using a previously published 3D velocity model (Rau and Wu, 1995) (Fig. 2). The seismicity distributed along the Western Foothills, the southern Central Range and the SE offshore Taiwan. South of the 2010 Jiashian earthquake source zone, a few earthquake clusters occurred along CCUF and in between CHNF and CCUF (Fig. 2). The 3D model of Rau and Wu (1995) was based on a damped, linear, least-squares inversion algorithm for simultaneous inversion of both a layered velocity model and the hypocentral locations (Eberhart-Phillips, 1993; Thurber, 1993). For the final inversion of the whole

Taiwan area, the weighted root mean square (WRMS) arrival time residuals were reduced by 36% from 0.271 s (initial) to 0.173 s (final). The average errors in absolute velocity of the final model range up to 0.04–0.08 km/s. We fixed the velocity model parameters and used the same algorithm of Rau and Wu (1995) to relocate the events. The average uncertainties of earthquake locations relocated by the 3D model are estimated to be 3 km horizontally and 5 km vertically. Although there are a few recent tomographic studies of Taiwan (e.g., Wu et al., 2007) using more recent data, the main features of the model do not differ much in comparison with those of Rau and Wu (1995), in particular in the inland area.

By incorporating first motions and *SH*/*P* amplitude ratios (Snoke et al., 1984), we determined focal mechanisms of earthquakes with $M_L \geq 3.0$ that occurred prior to June 2006 following the approach of Rau et al. (1996). For the events that occurred between June 2006 and March 2010, we used either the CMT or the first-motion solutions determined by the Central Weather Bureau for earthquakes with $M_L > 3.5$. This dataset also included 40 events associated with the 2010 Jiashian earthquake sequence. Focal mechanisms of the 40 events were determined using the genetic algorithm (Wu et al., 2008). The source parameters and the respective fault plane solutions of the 40 events are given in the supplementary data. A total of 466 focal mechanisms of small-to-moderate-sized events ($3.0 \leq M_L \leq 6.4$) in southwestern Taiwan between January 1991 and March 2010 were obtained in the present study.

We used T-TECTO 3.0 software (Žalohar and Vrabec, 2007, 2008, 2010) for the stress inversion of earthquake focal mechanism data. T-TECTO is based on the Gauss method (Žalohar and Vrabec, 2007, 2008, 2010) and effectively separates heterogeneous fault systems into homogeneous subsystems and thereby calculates the optimal stress tensors for each respective homogeneous subsystem. The results of stress inversion give the estimation of the orientation of the three principal stresses, where σ_1 is the maximum compressive stress, σ_2 is the intermediate compressive stress, and σ_3 is the minimum compressive stress. The stress ratio is defined as $D = (\sigma_2 - \sigma_3)/(\sigma_1 - \sigma_3)$.

In the following sections, we first present the results of relocated earthquakes, which are superposed on the tomographic model of Rau and Wu (1995), focusing on structures that might be related to the 2010 Jiashian earthquake sequence. Then, we examined focal mechanisms of the earthquakes and investigated the earthquake faulting and the responsible tectonic stress regime in and around the Jiashian earthquake sequence.

4. Relocated earthquakes and Tomography model

The relocated earthquakes, which were superimposed on to the tomographic model, are displayed in three E–W trending and three N–S trending profiles (Figs. 3 and 4). The selected profiles are chosen to show the major variations in velocity structures under southern Taiwan. In each of the plots, the white rectangular areas mark the unsampled regions with no resolution. The most prominent feature in the subsurface P-wave image is an east-dipping high velocity zone in the southernmost E–W profile C–C′ (8.0–8.4 km/s, or about 3–8% higher than the 1-D average model) from 25 to 30 km of depth in the west to 55–60 km depth in the east which coincides with the seismicity-defined Wadati–Benioff zone at a depth range of 30–80 km (the hatched area in Fig. 3). In the N–S profiles E–E′ and F–F′ (Fig. 4), we can observe the lower crustal seismicity (approximately 20–40 km depth), which disappears in the north part of the area in profile D–D′. We interpret this transition in seismicity to signify the northern limit of subducting Eurasian crust and lithosphere in southern Taiwan; this transition occurs at about the latitude of Kaohsiung City to the west and Lutao Island to the east (Fig. 2).

For better illustrate the tomographic structure which is likely related to the 2010 Jiashian earthquake we display tomography in depth-layer slices from surface to 80 km depth around the epicenter area (Fig. 5). The WNW–ENE-trending 2010 Jiashian earthquake sequence is roughly located along the northern edge of the subduction–collision transitional boundary and correlates with a E–W to WNW-trending high P-wave velocity bulge of 30-km wide and 40-km long at the 27 km depth-slice (Fig. 5). We tend to interpret this high P-wave velocity bulge as a result of buckling of the subducting Eurasian lithosphere, taking into account the location and the distribution of depth.

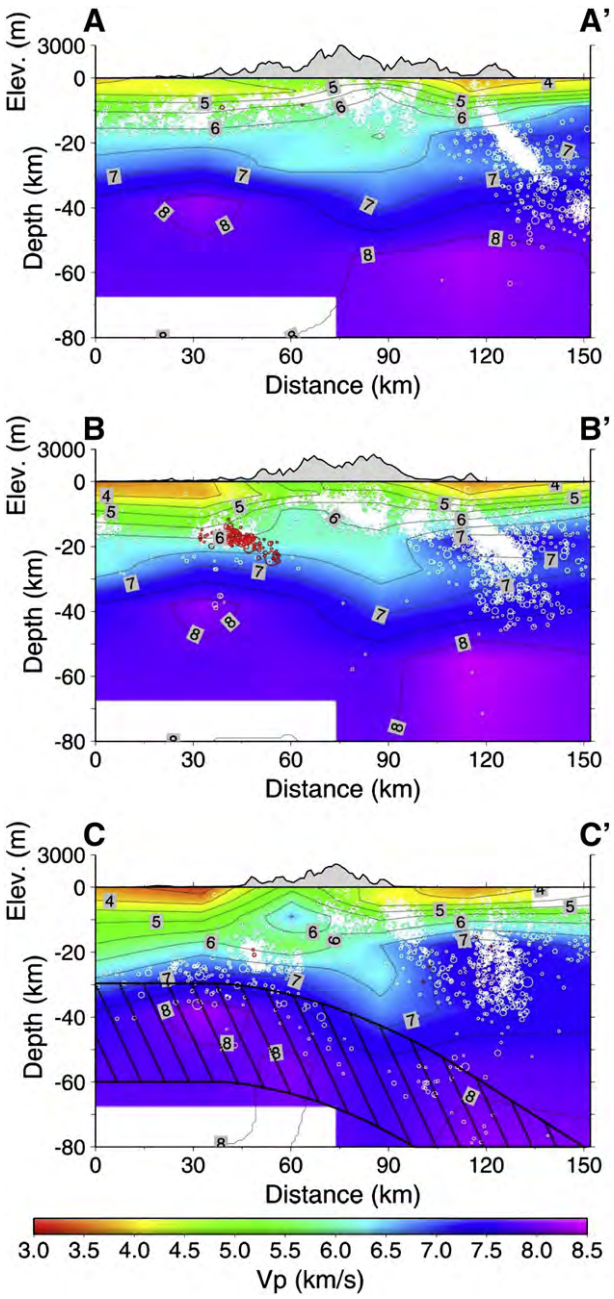

Fig. 3. P-wave velocity profiles AA′–CC′ in E–W direction (modified from Rau and Wu (1995)). The velocity contour interval is 0.5 km/s. The thickness for each cross section is ±12 km and the white circles are relocated hypocenters including events within 12 km distance of the profile (Fig. 2). The 2010 Jiashian mainshock–aftershocks are shown as red circles. The white area marks the unsampled regions. The seismicity-defined Wadati–Benioff zone; coincides with the inclined high velocity zone in profile CC′, is interpreted as the subducting lithosphere (the cross-hatched area). The topography corresponding to each profile is shown on top of the velocity section.

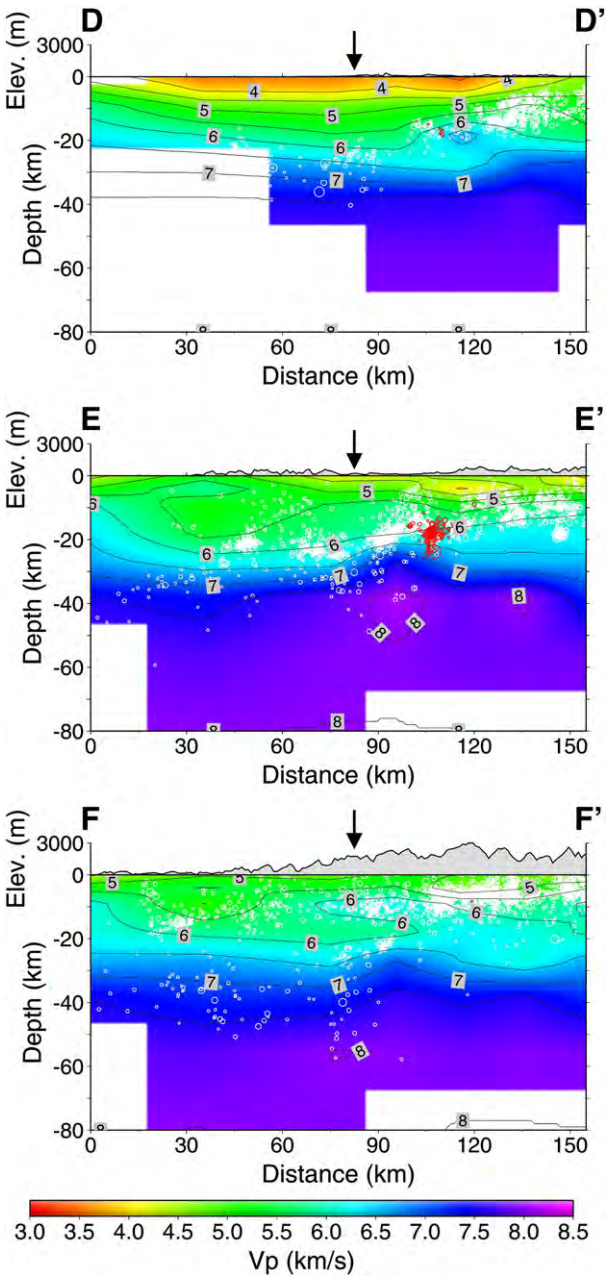

Fig. 4. P-wave velocity profiles DD′–FF′ in N–S direction. The velocity contour interval is 0.5 km/s. The thickness for each cross section is ±12 km and the white circles are relocated hypocenters including events within 12 km distance of the profile (Fig. 2). The 2010 Jiashian mainshock–aftershocks are shown as red circles. The white area marks the unsampled regions. The topography corresponding to each profile is shown on top of the velocity section.

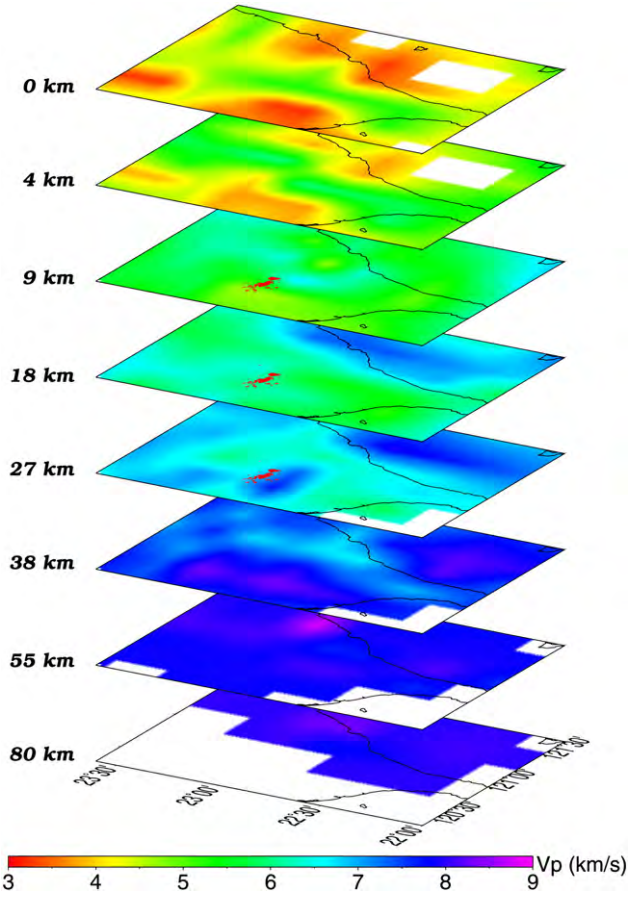

Fig. 5. A series of maps of southern Taiwan showing the P-wave velocity solutions at each layer for the results of 3D inversion (Rau and Wu, 1995). Red circles are the Jiashian earthquake sequence. The white area marks the unsampled regions. See text for further discussion.

5. Focal mechanisms

The results of focal mechanisms of 466 earthquakes show a mixture of thrust, strike–slip and normal faulting mechanisms in southwestern Taiwan (Fig. 6). P-axes of the thrust and strike–slip events are shown in Fig. 7. Thrust fault mechanisms with mostly E–W or ESE–WNW striking P-axes occur throughout the southern end of the Western Foothills with the focal depth extending at the shallow crustal level of 5–15 km and dipping to east–southeast. Around the Choukou thrust system (CKUF), the seismicity correlates spatially well to a 5–10 km east-dipping ramp (Fig. 8a). East of the Chukou fault and crossing from the fold-and-thrust belt to the slate belt, strike–slip fault mechanisms with a NW–SE striking P-axis and a NE–SW trending T-axis concentrate at 5–10 km shallow crustal level (Fig. 8a). The strike–slip events seemingly aligned in the E–W direction, implying an E–W trending left-lateral fault zone for about 10–12 km long. To the south, the cluster in the northern Chaochou fault (CCUF) (cross section BB′ in Fig. 6) is characterized by a mixture of thrust and normal faults with a likely high angle dip at the lower crustal level of 10–25 km depth (Fig. 8b).

The Jiashian earthquake sequence (cross section CC′ in Fig. 6) shows a combination of thrust and strike–slip fault mechanisms with the NE–SW striking P-axes (Figs. 7 and 8c). The angles of the P-axes of the Jiashian earthquake sequence events are significantly different and almost flip with 90° from the 20-year seismicity in the surrounding areas. Note that some pre-Jiashian events along the northern trace of the Chishan fault (CHNF), and west and southwest of the Jiashan cluster as well as directly south of the cluster, also show mechanisms with P-axes trending NE–SW. Taking the cross section perpendicular to the strike of the preferred nodal plane of the mainshock resulted from the CMT solution, we can clearly find that the aftershocks concentrate from 12 km to 25 km and dip 40–50° to the NE (Fig. 8c).

6. Stress inversions

For the stress tensor inversions, the 466 earthquake focal mechanism solutions were divided into six groups based on spatial clustering of the events in the study area (Fig. 9). By examining results of stress tensor inversion for each group, as expected from the style of

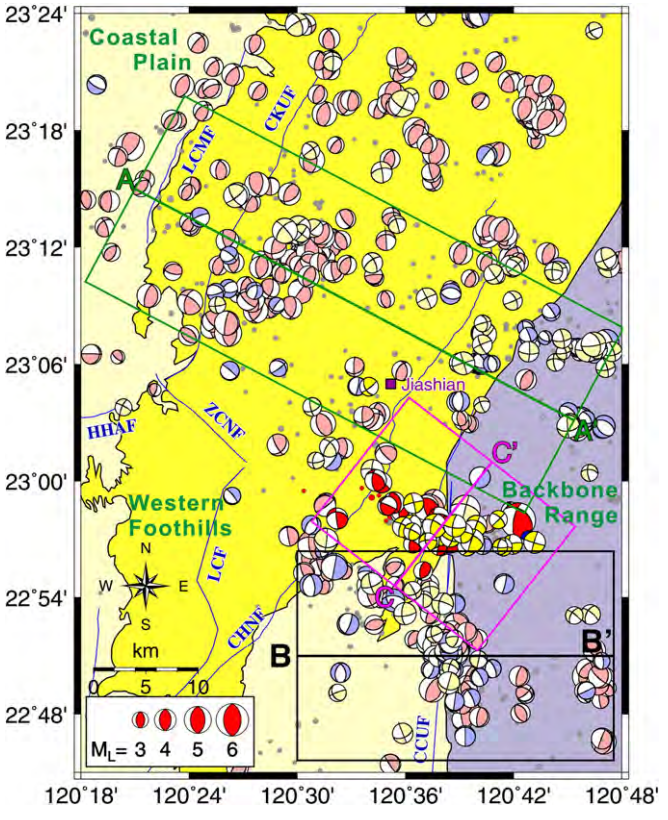

Fig. 6. Map of southwestern Taiwan showing 466 $3.0 \leq M_L \leq 6.4$ events with their focal mechanisms. On each focal sphere, the shaded area represents the compressive quadrant, and the white area represents the dilatational quadrant. The solutions are plotted on lower hemisphere, equal-area projection and are coded for magnitude (scale at lower right). The focal mechanisms of the 2010 Jiashian earthquake sequence are shown as red color for thrust, yellow for strike–slip and blue for normal fault mechanisms. The focal mechanisms of the background earthquakes are shown as pink color for thrust, light yellow for strike–slip and light blue for normal fault mechanisms. Active faults are shown as blue lines. Cross sections AA′–CC′ indicate the locations of the focal mechanisms plotted in back-hemisphere projection shown in Fig. 8. LCMF: Liuchia–Muchiliao fault; CKUF: Chukou fault; HHAF: Hsinhua fault; ZCNF: Zuochen fault; LCF: Lungchuan fault; CHNF: Chishan fault; CCUF: Chaochou fault.

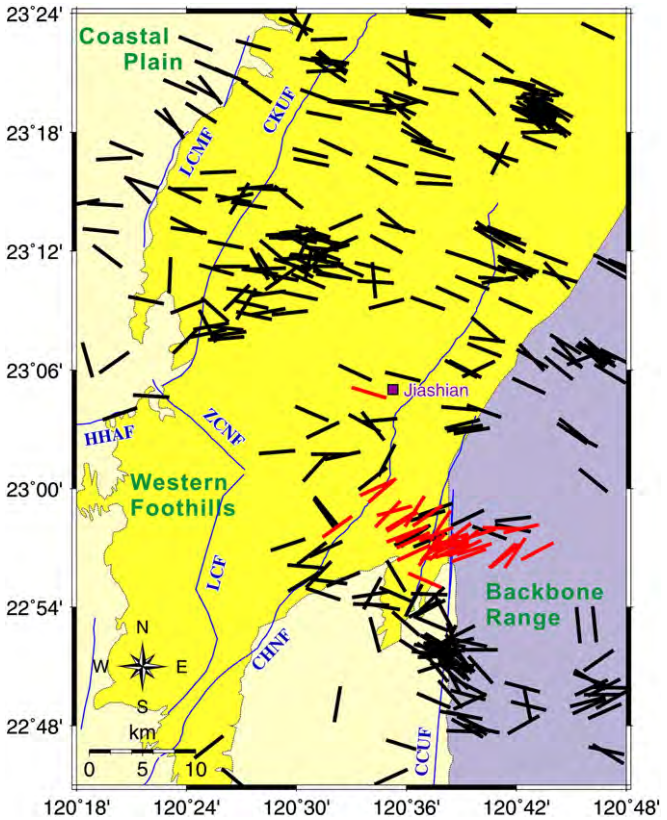

Fig. 7. Map of southwestern Taiwan showing the P-axes for both thrust and strike–slip mechanism events shown in Fig. 6. P-axes of the Jiashian earthquake sequence events are shown in red and the background earthquakes are shown in black. LCMF: Liuchia–Muchiliao fault; CKUF: Chukou fault; HHAF: Hsinhua fault; ZCNF: Zuochen fault; CHNF: Chishan fault; CCUF: Chaochou fault.

faulting of the earthquakes, the stress regime in southwestern Taiwan is characterized by a combination of thrust and strike–slip faulting regimes (i.e., transpression regime). The maximum principal stress, σ_1 is sub-horizontal, however, revealing a variation of orientations in different sub-areas. For the southern Foothills areas northwest away from the Jiashian earthquake sequence zone (groups A, B and C) more than 90% of the events can be described by pure thrust faulting regime with σ_1 trending either E–W or NW–SE. East of the southern Foothills (group D), crossing from the fold-and-thrust belt to the slate belt and north of the Jiashian sequence zone, indicates a dominant strike–slip faulting regime with the same orientation of σ_1 trending NW–SE and σ_3 oriented NE–SW. In the northern Chaochou fault (group F) south of the Jiashian sequence zone, where the style of faulting is characterized by an intriguing mixture of thrust, strike–slip and normal faults, the resultant stress tensor is consistent with a NW–SE trending σ_1 and NE–SW oriented σ_3 stress regime. For the area of the Jiashian earthquake sequence (group E), unlike the aforementioned surrounding areas, the inverted stress tensor shows a thrust faulting regime with σ_1 trending ENE–WSW, which is a difference of nearly 90°. Considering the Jiashian earthquake sequence alone, more than 98% of the events are consistent with an oblique strike–slip faulting regime with minor thrusting, with σ_1 trending NE–SW and σ_3 oriented NW–SE. This indicates a local deviation of more than 90° in σ_1 orientation comparing the stress tensor of the Jiashian earthquake sequence with its surroundings.

7. Discussion

The most prominent feature of the earthquake focal mechanisms and inverted stress state of the 2010 M_L 6.4 Jiashian earthquake sequence is that both P-axes and σ_1 of the Jiashian events are oriented sub-parallel to the strike of the orogen, which differ from neighboring events whose σ_1 are in general orogen-perpendicular and consistent with the plate convergence direction. In comparison with the other parts of southern Taiwan, the 2010 Jiashian earthquake with orogen-parallel P-axis appears to be the only odd for all the $M>5.5$ events occurred in southern Taiwan. This uncommon feature is very different from that found in NE Taiwan where frequent moderate-size earthquakes with orogen-parallel P-axes have been observed (Kao et al., 1998). Note that the Ryukyu trench almost strikes perpendicular to the local trend of the Taiwan orogen in NE Taiwan, the Ryukyu slab acts effectively as a stress guide to transmit the effects of Taiwan collision laterally through the subducted Philippine Sea plate in the subduction–collision transition zone (Kao and Rau, 1999; Kao et al., 1998). Unlike the transition zone in NE Taiwan, the obliquity between the NNW–SSE-striking subducted Eurasian plate and the N–S turn NNE–SSW-oriented orogen trend in southern Taiwan is about 35° (Fig. 1). Given the relatively small subduction obliquity and the fact that no moderate-size event with orogen-parallel P-axis occurred in southern Taiwan pre-Jiashian, Kao et al. (2000) concluded that the lateral compression of Taiwan collision are not significant in the southern Taiwan subduction–collision transition zone, as compared to that in NE Taiwan. With the appearances of

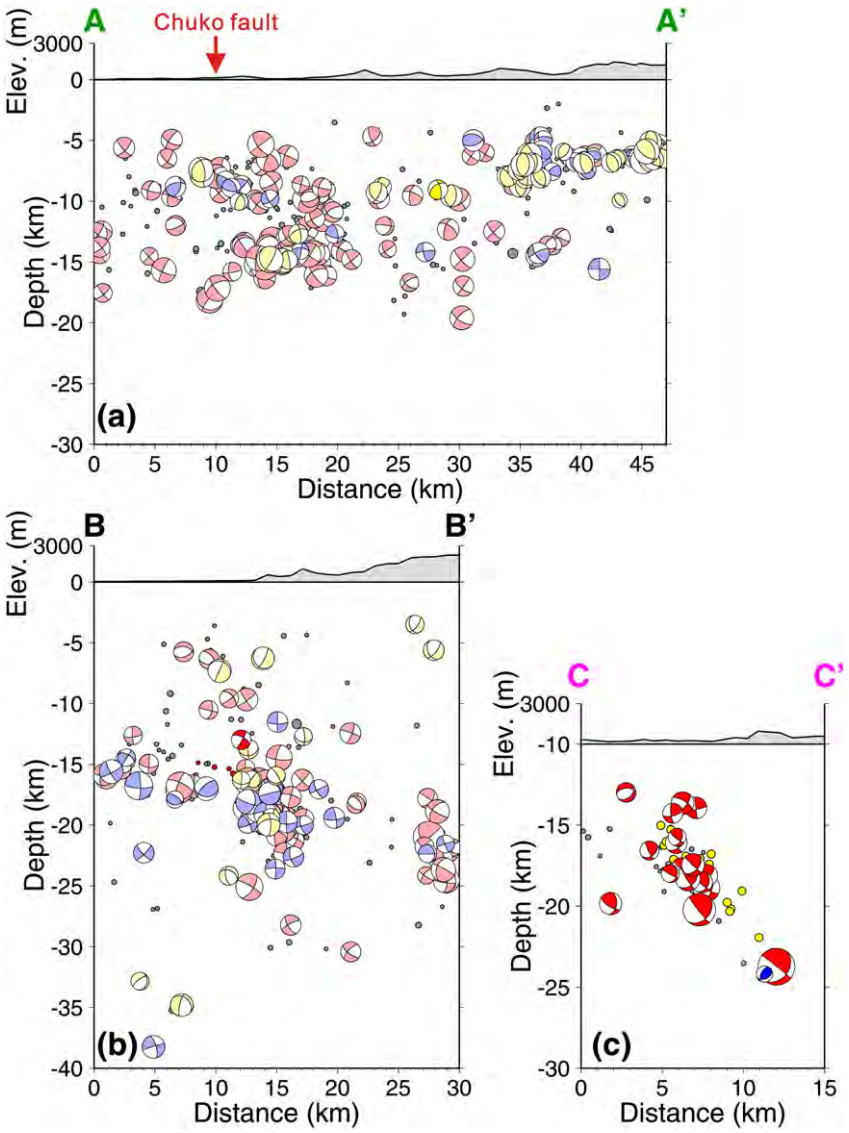

Fig. 8. Cross sections showing the focal mechanisms plotted in back-hemisphere projection. Locations of the cross sections are indicated in Fig. 6. The topography corresponding to each profile is shown on top of the cross section.

the 2010 M_L 6.4 Jiashian earthquake sequence, however, we find that the collision-related lateral compression does exist in the subduction terminus of the southern Taiwan, just as not frequent as those found in NE Taiwan. Furthermore, some pre-Jiashian events located south and southwest of the Jiashian earthquake sequence showing mechanisms with P-axes directing NE–SW, although unnoticed beforehand, have foreseen lateral compression in the southern Taiwan subduction–collision transition zone.

It appears that the NE-trending σ_1 is only derived from the earthquakes (including the seismicity and the Jiashian sequence) near the NW-trending Jiashian earthquake sequence zone, which seemingly correspond the regional geological structure of the Chishan transfer fault zone, a step-over connection between the major NNE-trending thrust faults in fold-and-thrust belt. As a result, we propose another possible interpretation for this nearly 90° difference of σ_1 orientation. We argue that there is a local stress deviation around the Chishan transfer fault zone under a regional NW to WNW-trending contraction in the southwestern Taiwan. It is rather common that the compressive stress tends to turn perpendicular to the major structures. For instance, we found a fan shape distribution of σ_1 in the 400-km long Taiwan mountain belt, which also shows fan shape main structure grain from north to south (Angelier et al., 1986). In the study area of southwestern Taiwan, the regional NW to WNW compressive stress is in generally perpendicular to the regional NNE major structures. We interpret that this regional compressive stress turns about 90° when it encounters the oblique NW-trending Chishan transfer fault zone, so the compressive stress would be perpendicular to Chishan transfer fault zone.

Superimposing the distribution of the Jiashian aftershocks and pre-Jiashian events onto the coseismic source model derived from GPS observations (Ching et al., 2011), three distinct seismic clusters can be identified in and near the source zone (Fig. 10). With the improvement of earthquake relocations, in comparison with those of Ching et al. (2011), our relocated seismicity appears to be more organized and in better agreement with the coseismic source model. In the area of the Jiashian earthquake (i.e., not including the shallow earthquakes NE of this area) we recognize three clusters of earthquakes. Two of the clusters, one at ~23 km and the other ranging from 13 to 21 km, are mainly defined by aftershocks and delineate the northeast dipping Jiashian seismic zone; the shallower cluster is also concentrated along the bottom of the coseismic source zone interpreted from GPS data (Fig. 10; Ching et al., 2011). The third cluster, located southwest of the source area, is composed of pre-Jiashian events and contain many P-axes that trend NE–SW. The latter two

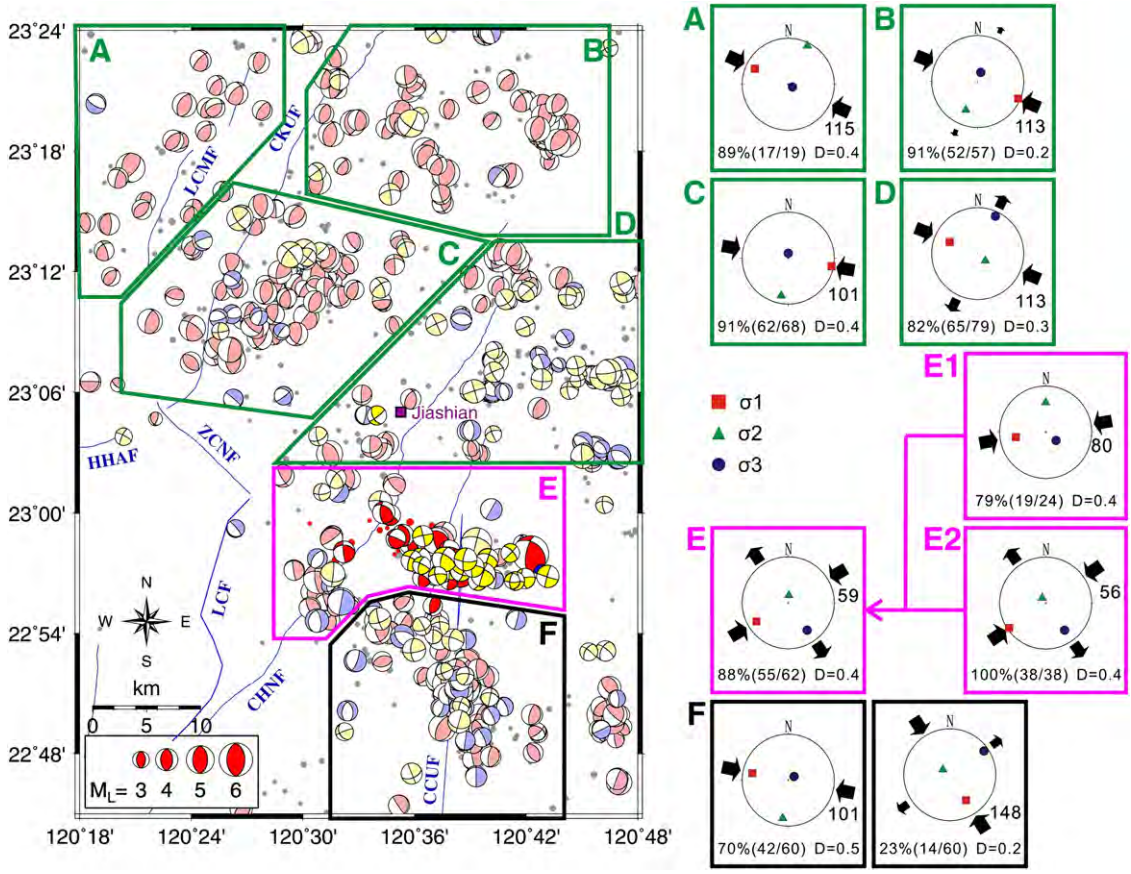

Fig. 9. Map of southwestern Taiwan showing the focal mechanisms of 466 $3.0 \leq M_L \leq 6.4$ events and their stress inversion results. The focal mechanisms are divided into six groups A–F based on their spatial clustering in southwestern Taiwan. The best-fit solutions of each stress inversion are shown in the stereonet for the orientations of σ_1 (red square), σ_2 (green triangle) and σ_3 (blue circle). The percentage of data satisfying the best-fit solution and the corresponding D value are shown below each stereonet. The orientation of best-fit σ_1 is indicated in each stereonet. Active faults are shown as blue lines. LCMF: Liuchia–Muchiliao fault; CKUF: Chukou fault; HHAF: Hsinhua fault; ZCNF: Zuochen fault; LCF: Lungchuan fault; CHNF: Chishan fault; CCUF: Chaochou fault. See text for further discussion.

clusters are also concentrated near the bottom of the seismic–aseismic transition in this area (~15 km, Fig. 8a). In terms of the time scenario of the two Jiashian mainshock–aftershock clusters, the Jiashian earthquake nucleated at a depth of ~23 km and propagated 40° up-dip in the WNW direction and terminated upward at a depth of 10 km. The concealed blind fault is interpreted to represent lateral ramp with oblique slip, which connects stepping major thrust faults in the fold-and-thrust belt (Ching et al., 2011). The extension of the rupture upward to the surface roughly corresponds to the southeast extension of the Zuochen fault or the Chishan transfer fault zone (Fig. 10) (Ching et al., 2011), however, no direct earthquake-related surface rupture was found. Consequently, the 2010 Jiashian earthquake once again underscores the seismic hazard of concealed fault, which have drawn worldwide attention (Shaw and Shearer, 1999).

Other than the 2010 Jiashian earthquake sequence mentioned above, all the seismic clusters in the study area (Figs. 6–9) reveal a consistent NW to WNW directed contraction, showing either pure contraction regime (thrust faulting) with σ_1 trending either E–W or NW–SE (southern Foothills areas, groups A, B and C of Fig. 9), or a pure strike–slip faulting regime with σ_1 trending NW–SE and σ_3 oriented NE–SW (east of the southern Foothills, group D of Fig. 9), or transpression regime (thrust/strike–slip faulting) with σ_1 trending NW–SE and σ_3 oriented NE–SW (northern Chaochou fault, group F of Fig. 9). Not surprising, the NW–SE-trending σ_1 is in general consistent with the plate convergence direction. Thrust fault mechanisms throughout the southern end of the Western Foothills at shallow crustal level represent frontal thrusts in the fold-and-thrust belt. In eastern end of the fold-and-thrust belt to the slate belt, strike–slip faults appear to be reactivated from pre-existing E–W trending normal faults, which were widespread in southwestern Taiwan during Miocene pre-collision state (Lee and Chan, 2007; Lin and Watts, 2002). The cluster in the northern Chaochou fault at the lower crustal level of 10–25 km depth (cross section BB′ in Fig. 6 and Fig. 8b), is characterized by a mixture of thrust, strike–slip and normal faulting. The thrust and strike–slip faulting mechanisms represent the plate convergence and we tend to interpret that the normal faulting is caused by flexure resulted from bending of the Eurasian subducting plate. It is clear that interaction of extensional and compressional stress regimes is occurring in southern Taiwan, which might be closely related to the subducting Eurasia (South China Sea) slab.

8. Conclusions

Analysis of seismic tomography and 20-year seismicity indicates that the 2010 M_L 6.4 Jiashian earthquake sequence is located at the subduction–collision transition zone in southern Taiwan. Focal mechanisms and stress state studies show that the P-axes of the 2010 Jiashian earthquake sequence are orogen-parallel, implying the effects of collision-related lateral compression exist in southern Taiwan, although an alternative interpretation of local stress deviation is possible. The areas surrounding the Jiashian sequence, however, show σ_1 is in general consistent with the plate convergence direction. The 2010 Jiashian earthquake apparently corresponds to the Chishan transfer fault zone, a lateral ramp or step-over connecting the major

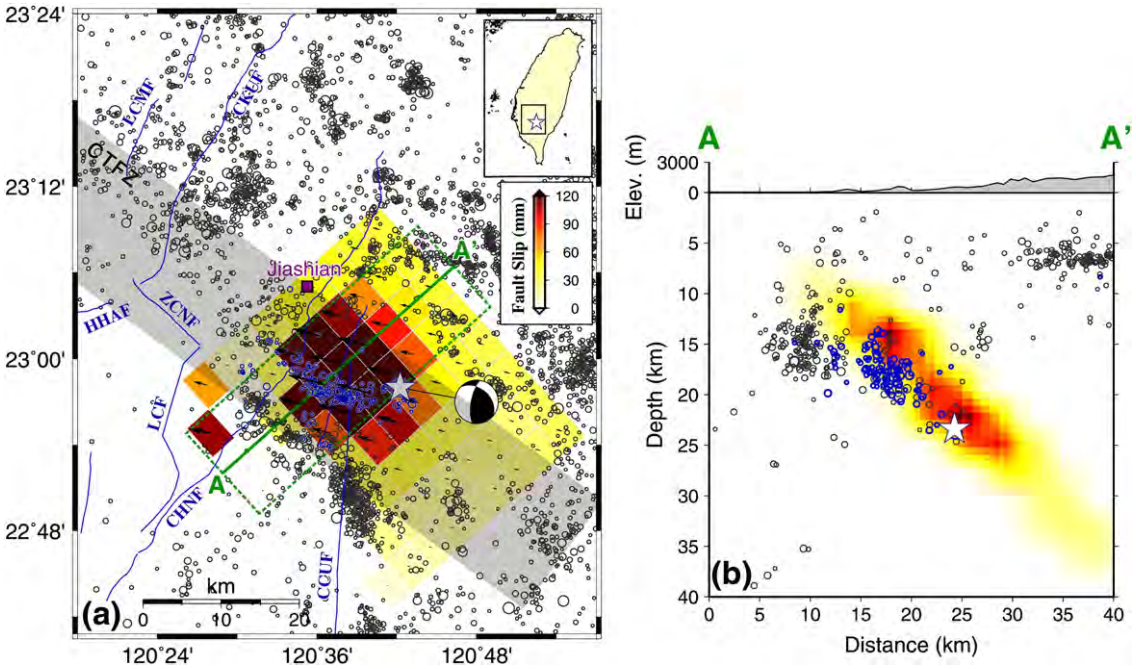

Fig. 10. (a) Map view of southwestern Taiwan showing the GPS-derived coseismic slip model for the 2010 M_L 6.4 Jiashian event (Ching et al., 2011), compared to the distributions of the Jiashian aftershocks (blue circles) and the background seismicity (black circles). The Jiashian mainshock is shown as a white star with the focal mechanism. Active faults are shown as blue lines. LCMF: Liuchia–Muchiliao fault; CKUF: Chukou fault; ZCNF: HHAF: Hsinhua fault; Zuochen fault; LCF: Lungchuan fault; CHNF: Chishan fault; CCUF: Chaochou fault. Chishan transfer fault zone (CTFZ) is shown as a shaded zone. Insert shows the map of Taiwan with the study area in black rectangle. (b) Northeast striking cross section A–A′ showing both the Jiashian aftershocks (blue circles) and the background seismicity (black circles). The Jiashian mainshock is shown as a white star. The topography corresponding to the profile is shown on top of the section.

thrust faults. On the other hand, this transfer fault zone and the Jiashian earthquake fault is not obviously related to any mapped surface geological structure. The result highlights the importance of seismic hazard of buried fault.

Acknowledgements

We thank the Seismological Center of Central Weather Bureau of Taiwan for the earthquake data. We are grateful to the Editor and two anonymous reviewers for their constructive comments on the manuscript. Figures were generated using the Generic Mapping Tools (GMT), developed by Wessel and Smith (1991). This research was partially supported by Taiwan NSC grant 99-2116-M-006-020.

Appendix A. Supplementary data

Supplementary data to this article can be found online at doi:10.1016/j.tecto.2011.09.013.

References

Angelier, J., Barrier, E., Chu, H.-T., 1986. Paleostress trajectories related to plate collision in the Foothills fold-thrust belt of Taiwan. Tectonophysics 125, 161–178.
Chi, W.R., Huang, H.M., 1981. Nannobiostratigraphy and paleo-environments of the late Neogene sediments and their tectonic implications in the Miaoli area, Taiwan. Pet. Geol. Taiwan 18, 111–129.
Ching, K.-E., Rau, R.-J., Lee, J.-C., Hu, J.-C., 2007. Contemporary deformation of tectonic escape in SW Taiwan from GPS observations, 1995–2005. Earth and Planetary Science Letters 262, 601–619. doi:10.1016/j.epsl.2007.08.017.
Ching, K.-E., Johnson, K.M., Rau, R.-J., Chuang, R.Y., Kuo, L.-C., Leu, P.-L., 2011. Inferred Fault geometry and slip distribution of the 2010 Jiashian, Taiwan, earthquake is consistent with a thick-skinned deformation model. Earth and Planetary Science Letters 301, 78–86. doi:10.1016/j.epsl.2010.10.021.
Deffontaines, B., Lee, J.-C., Angelier, J., Carvalho, J., Rudant, J.-P., 1994. New geomorphic data on the active Taiwan orogen: a multisource approach. Journal of Geophysical Research 99 (B10), 20,243–20,266.
Deffontaines, B., Lacombe, O., Angelier, J., Chu, H.T., Mouthereau, F., Lee, C.T., Deramond, J., Lee, J.F., Yu, M.S., Liew, P.M., 1997. Quaternary transfer faulting in the Taiwan Foothills: evidence from a multisource approach. Tectonophysics 274, 61–82.
Eberhart-Phillips, D., 1993. Local earthquake tomography: earthquake source regions. In: Iyer, H.M., Hirahara, K. (Eds.), Seismic Tomography: Theory and Practice. Chapman and Hall, London, pp. 614–643.
Hu, J.C., Angelier, J., Lee, J.C., Chu, H.T., Byrne, D., 1996. Kinematics of convergence, deformation and stress distribution in the Taiwan collision area: 2-D finite-element numerical modeling. Tectonophysics 255, 243–268.
Kao, H., Rau, R.-J., 1999. Detailed structures of the subducted Philippine Sea plate beneath northeast Taiwan: A new type of double seismic zone. Journal of Geophysical Research 104, 1015–1033.
Kao, H., Shen, S.J., Ma, K.F., 1998. Transition from oblique subduction to collision: earthquakes in the southernmost Ryukyu arc-Taiwan region. Journal of Geophysical Research 103, 7211–7230.
Kao, H., Huang, G.C., Liu, C.S., 2000. Transition from oblique subduction to collision in the northern Luzon arc-Taiwan region: constraints from bathymetry and seismic observations. Journal of Geophysical Research 105, 3059–3079.
Lacombe, O., Mouthereau, F., Deffontaines, B., Angelier, J., Chu, H.T., Lee, C.T., 1999. Geometry and Quaternary kinematics of fold-and-thrust units of southwestern Taiwan. Tectonics 18, 1198–1223.
Lacombe, O., Mouthereau, F., Angelier, J., Deffontaines, B., 2001. Structural, geodetic and seismological evidence for tectonic escape in SW Taiwan. Tectonophysics 333, 323–345.
Lee, J.C., Chan, Y.C., 2007. Structure of the 1999 Chi-Chi earthquake rupture and interaction of thrust faults in the active fold belt of western Taiwan. Journal of Asian Earth Sciences 31, 226–239.
Lin, A.-T., Watts, A.B., 2002. Origin of the West Taiwan Basin by orogenic loading and flexure of a rifted continental margin. Journal of Geophysical Research 107, 2185. doi:10.1029/2001JB000669.
Rau, R.-J., Wu, F.T., 1995. Tomographic imaging of lithospheric structures under Taiwan. Earth and Planetary Science Letters 133, 517–532.
Rau, R.-J., Wu, F.T., Shin, T.C., 1996. Regional network focal mechanism determination using 3-D velocity model and SH/P amplitude ratio. Bulletin of the Seismological Society of America 86, 1270–1283.
Rau, R.-J., Ching, K.-E., Hu, J.-C., Lee, J.-C., 2008. Crustal deformation and block kinematics in transition from collision to subduction: GPS measurements in northern Taiwan, 1995–2005. Journal of Geophysical Research 113, B09404. doi:10.1029/2007JB005414.
Seno, T., 1977. The instantaneous rotation vector of the Philippine Sea plate relative to the Eurasian plate. Tectonophysics 42, 209–226.
Seno, T., Stein, S., Gripp, A.E., 1993. A model for the motion of the Philippine sea plate consistent with NUVEL-1 and geological data. Journal of Geophysical Research 98, 17,941–17,948.

Shaw, J.H., Shearer, P.M., 1999. An elusive blind-thrust fault beneath metropolitan Los Angeles. Science 283 (5407), 1516–1518.
Shyu, J.B., Sieh, K., Chen, Y.G., Liu, C.S., 2005. Neotectonic architecture of Taiwan and its implications for future large earthquakes. Journal of Geophysical Research 110, B08402. doi:10.1029/2004JB003251.
Snoke, J.A., Munsey, J.W., Teague, A.G., Bollinger, G.A., 1984. A program for focal mechanism determination by combined use of polarity and SV-P amplitude ratio data. Earthquake Notes 55, 15.
Suppe, J., 1981. Mechanics of mountain building and metamorphism in Taiwan. Memorial Geological Society China 4, 67–89.
Suppe, J., 1984. Kinematics of arc–continent collision, flipping of subduction and back-arc spreading near Taiwan. Memorial Geological Society China 6, 21–33.
Teng, L.S., 1979. Petrographical study of the Neogene sandstones of the Coastal Range, eastern Taiwan (I. Northern part). Acta Geological Taiwan 20, 129–156.
Teng, L.S., Lee, C.T., 1996. Geomechanical appraisal of seismogenic faults in northeast Taiwan. Journal Geological Society China 39, 125–142.
Thurber, C.H., 1993. Local earthquake tomography: velocities and Vp/Vs-Theory. In: Iyer, H.M., Hirahara, K. (Eds.), Seismic Tomography: Theory and Practice. Chapman and Hall, London, pp. 563–583.
Wessel, P., Smith, W., 1991. Free software helps map and display data. Eos Transaction AGU 72 (441), 445–446.
Wiltschko, D.V., Hassler, L., Hung, J.H., Liao, H.S., 2010. From accretion to collision: motion and evolution of the Chaochou Fault, southern Taiwan. Tectonics 29. doi:10.1029/2008TC002398 TC2015.
Wu, F.T., Rau, R.-J., 1998. Seismotectonics and identification of potential seismic source zones in Taiwan. Terrestrial, Atmospheric and Oceanic Sciences 9, 739–754.
Wu, Y.M., Chang, C.H., Zhao, L., Shyu, J.B.H., Chen, Y.G., Sieh, K., Avouac, J.P., 2007. Seismic tomography of Taiwan: improved constraints from a dense network of strong-motion stations. Journal of Geophysical Research 112, B08312. doi:10.1029/2007JB004983.
Wu, Y.M., Zhao, L., Chang, C.H., Hsu, Y.J., 2008. Focal-mechanism determination in Taiwan by genetic algorithm. Bulletin of the Seismological Society of America 98, 651–661. doi:10.1785/0120070115.
Yang, C.-C.B., Chen, W.-S., Wu, L.-C., Lin, C.-W., 2007. Active deformation front delineated by drainage pattern analysis and vertical movement rates, southwestern Coastal Plain of Taiwan. Journal Asian Earth Science 31, 251–264.
Yang, K.-M., Huang, S.-T., Wu, J.-C., Ting, H.H., Mei, W.-W., 2006. Review and new insights on foreland tectonics in western Taiwan. International Geology Review 48, 910–941.
Yu, S.B., Chen, H.Y., Kuo, L.C., 1997. Velocity field of GPS Stations in the Taiwan area. Tectonophysics 274, 41–59.
Žalohar, J., Vrabec, M., 2007. Paleostress analysis of heterogeneous fault-slip data: the Gauss method. Journal of Structural Geology 29, 1798–1810. doi:10.1016/j.jsg.2007.06.009.
Žalohar, J., Vrabec, M., 2008. Combined kinematic and paleostress analysis of fault-slip data: the Multiple-slip method. Journal of Structural Geology 30, 1603–1613. doi:10.1016/j.jsg.2008.09.004.
Žalohar, J., Vrabec, M., 2010. Kinematics and dynamics of fault reactivation: the Cosserat approach. Journal of Structural Geology 32, 15–27. doi:10.1016/j.jsg.2009.06.008.